

# Relation between coupled-mode theory and equivalent layers for multilayer interference coatings

Nicolai Matuschek, Günter Steinmeyer, and Ursula Keller

The method of equivalent layers is a commonly used technique for designing optical multilayer interference coatings. Herpin's theorem [C. R. Acad. Sci. **225**, 182 (1947)] states that every symmetrical multilayer structure is equivalent, at one arbitrary wavelength, to a single homogeneous layer. The Herpin equivalent layer is described by two design parameters, the equivalent index and the equivalent thickness. Alternatively, we recently developed an exact coupled-mode analysis for the description of multilayer interference coatings composed of a symmetrical combination of layers. The design parameters of the coupled-mode theory are the exact coupling coefficient and the exact detuning coefficient. Recently we used this method in the design of chirped mirrors for dispersion compensation. We prove that the two methods are equivalent and derive relations that link the design parameters of both formalisms. By use of these relations it is possible to translate between the coupled-mode formalism and the method of equivalent layers. The simultaneous availability of both design methods gives a new perspective on the analytical design of optical interference coatings with challenging spectral response characteristics. © 2000 Optical Society of America

OCIS codes: 310.1620, 310.6860.

## 1. Introduction

One of the most powerful analytical design tools in the theory of thin-film optical coatings is the method of equivalent layers. According to Herpin's theorem, every symmetrical multilayer structure is equivalent, at one arbitrary wavelength, to a single homogeneous layer.<sup>1</sup> This layer, called the equivalent layer, is characterized by its equivalent (refractive) index  $N_e$  (Herpin index) and its equivalent (phase) thickness  $\Gamma_e$ . For the design wavelength, the replacement of multiple layers by an equivalent layer conserves the optical properties of the coating and is therefore exact. Adjustment of  $N_e$  and  $\Gamma_e$  allows for the analytical design of multilayer coatings with various constraints on their spectral response characteristics.<sup>2-7</sup>

An alternative description of multilayer coatings uses the coupled-mode theory. Originally, this ap-

proach described weakly index-modulated systems such as waveguides,<sup>8,9</sup> (chirped) fiber gratings,<sup>10</sup> and distributed-feedback lasers.<sup>11</sup> The coupled-mode equations are a differential equation system for the rightward- and leftward-propagating waves. The solution of this differential equation system results in a transfer matrix that relates waves at different positions, both inside and outside the multilayer structure. In coupled-mode theory the design parameters are the coupling coefficient  $\kappa$  and the detuning coefficient  $\delta$ . For systems with weak index modulation the standard coupled-mode approach provides an excellent approximation to the problem. In contrast, for the design of dielectric multilayer filters and mirrors, standard coupled-mode theory is regarded as insufficient because the assumption of a small perturbation is violated in the case of large index discontinuities. However, we recently proved that by proper redefinition of the design parameters the coupled-mode theory can be made absolutely exact even for the description of multilayer interference coatings with arbitrarily large refractive-index differences.<sup>12</sup>

In both exact formalisms, the symmetrical multilayer structure is described by a set of two wavelength-dependent design parameters. Using these wavelength-dependent parameters in the respective formalism permits the calculation of the spectral response characteristics of the multilayer coating. One might assume that there is a closer

---

The authors are with the Ultrafast Laser Physics Laboratory, Institute of Quantum Electronics, Swiss Federal Institute of Technology, Zürich Eidgenössische Technische Hochschule (ETH), ETH Hönggerberg HPT E12, CH-8093 Zürich, Switzerland. G. Steinmeyer's e-mail address is sguenter@iqe.phys.ethz.ch.

Received 27 September 1999; revised manuscript received 21 December 1999.

0003-6935/00/01626-07\$15.00/0

© 2000 Optical Society of America

connection between coupled-mode theory and the method of equivalent layers. In this paper we investigate the relationship between the two methods and derive relations that link the parameters of coupled-mode theory ( $\kappa$ ,  $\delta$ ) with those that describe the equivalent layer ( $N_e$ ,  $\Gamma_e$ ). As a result, we find that the equivalent thickness is a linear function of  $\gamma$ , the exact effective propagation constant of the Bragg structure.

The coupled-mode equations can be converted into equivalent transmission-line equations.<sup>13,14</sup> For these transmission-line equations a normalized characteristic impedance  $Z$  is defined and can be expressed as a function of the coupling and detuning coefficients. We find that the equivalent index is proportional to the reciprocal characteristic impedance, i.e.,  $N_e \propto Z^{-1}$ .

The relations between the design parameters permit switching between the coupled-mode formalism and the method of equivalent layers, and the results derived within one formalism can be transformed into the other. The specific design problem dictates which method would be more convenient. As an example, if phase properties of the multilayer coating are a primary concern, the coupled-mode approach is advantageous, whereas if matching of refractive index and phase thickness is more important, the method of equivalent layers is favored.

In Subsection 2.A we review the method of characteristic matrices and its connection to the equivalent layers in the case of arbitrary, symmetrical multilayer structures. Subsection 2.B deals with the transfer-matrix method and exact coupled-mode equations, as derived in Ref. 12. In Subsection 2.C the characteristic matrix is related to the transfer matrix. From this we get the link between coupled-mode theory and the equivalent layer, and it is then straightforward to derive the relations between the parameters ( $\kappa$ ,  $\delta$ ) and ( $N_e$ ,  $\Gamma_e$ ). We apply these results to the most important case, the case of the symmetrical three-layer combination, and, using contour plots, discuss the behavior of the design parameters (Section 3).

## 2. Theory

### A. Characteristic Matrix and Equivalent Layers

We consider a symmetrical combination of nonabsorbing, homogeneous layers. The propagation of light is assumed to be perpendicular to the stratified medium. A special case is the three-layer combination in Fig. 1. It should be noted that the equations of Section 2 are applicable to any symmetrical layer combination with an arbitrary number of layers.

The electric and magnetic fields at the beginning and the end of the layer combination are related by the equation

$$\begin{pmatrix} E_l \\ H_l/Y_0 \end{pmatrix} = \begin{bmatrix} M_{11} & iM_{12} \\ iM_{21} & M_{11} \end{bmatrix} \begin{pmatrix} E_r \\ H_r/Y_0 \end{pmatrix}, \quad (1)$$

where the characteristic-matrix elements  $M_{ij}$  are real quantities.<sup>5,6</sup> The symmetry of the multilayer struc-

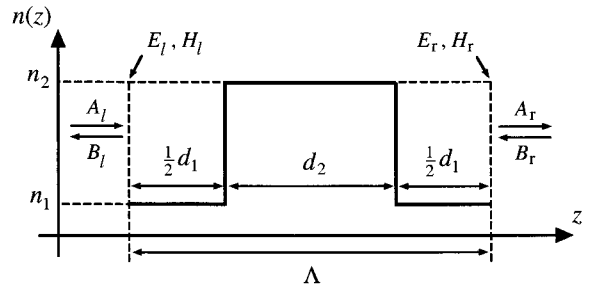


Fig. 1. Refractive-index profile of a symmetrical combination of three homogeneous layers. The optical phase shift of each outer layer (medium 1) is  $\phi_1/2$ , with  $\phi_1 = kn_1d_1$ , and the optical phase shift of the center layer (medium 2) is  $\phi_2 = kn_2d_2$ . Here  $k$  is the vacuum wave number,  $n_{1/2}$  is the refractive index of medium 1/2, and  $d_{1/2}$  is the corresponding physical layer thickness ( $\Lambda = d_1 + d_2$ ). The sum of the phase variables,  $\phi = \phi_1 + \phi_2$ , defines the total optical phase shift of the three-layer combination; the difference of the phase variables,  $\Delta\phi = \phi_2 - \phi_1$ , is a measure of the duty cycle. The amplitudes  $E_{l/r}$  and  $H_{l/r}$  denote the electric and the magnetic fields, respectively, and  $A_{l/r}$  and  $B_{l/r}$  represent the traveling waves in the right and left directions on the left and right ends, respectively, of the multilayer structure.

ture results in equal diagonal matrix elements, i.e.,  $M_{11} = M_{22}$ . In Eq. (1),  $E_{l/r}$  and  $H_{l/r}$  are the electric and the magnetic fields on the left and the right ends of the symmetrical combination of layers, respectively (see Fig. 1). The quantity  $Y_0 \approx 2.65 \times 10^{-3} \Omega^{-1}$  denotes the optical admittance of free space. The characteristic matrix does not contain any information about the surrounding media; it contains no information about the refractive index of adjacent layers, the substrate material, or the ambient medium.

The characteristic matrix of the layer combination in Eq. (1) is of the same structure as the characteristic matrix of a single homogeneous layer. Therefore, for one arbitrary wavelength, this matrix can be replaced by the matrix of Herpin's equivalent single layer:

$$\mathbf{M}_e = \begin{bmatrix} \cos(\Gamma_e) & \frac{i}{N_e} \sin(\Gamma_e) \\ iN_e \sin(\Gamma_e) & \cos(\Gamma_e) \end{bmatrix}. \quad (2)$$

By comparison of matrices in Eqs. (1) and (2) the equivalent-layer parameters are defined by the elements of the characteristic matrix:

$$N_e = \sqrt{M_{21}/M_{12}}, \quad (3)$$

$$\cos(\Gamma_e) = M_{11}. \quad (4)$$

According to Eq. (4), the equivalent index and the equivalent thickness are real quantities if  $|M_{11}| \leq 1$ . This condition defines the passband regions of the multilayer coating. In contrast, for  $|M_{11}| > 1$  the equivalent-layer parameters become complex, and these regions are called stop bands. Obviously, the inversion of Eq. (4) results in a multivalued solution for  $\Gamma_e$ . The equivalent thickness is defined as that value nearest the total phase thickness  $\phi$  that corre-

sponds to the total optical thickness of the symmetrical combination of layers (see Fig. 1).<sup>5</sup> More precisely,  $\Gamma_e$  has to be chosen such that its real part is a continuous, monotone nondecreasing function of the vacuum wave number  $k$  with  $\Gamma_e(k = 0) = 0$ .<sup>2</sup>

### B. Transfer Matrix and Exact Coupled-Mode Theory

In what follows, we use the results derived in Ref. 12 for the transfer matrix of one period of an arbitrary combination of layers. The transfer matrix connects the field amplitudes of the rightward- and leftward-traveling waves at the beginning and the end of the multilayer structure according to

$$\begin{pmatrix} A_l \\ B_l \end{pmatrix} = \mathbf{T} \begin{pmatrix} A_r \\ B_r \end{pmatrix}. \quad (5)$$

Here  $A_{l/r}$  and  $B_{l/r}$  are the normalized amplitudes of the right- and left-traveling waves on the left and the right ends of the layer combination, respectively (see Fig. 1). For nonabsorbing layers, the transfer matrix  $\mathbf{T}$  is of the general form

$$\mathbf{T} = \begin{bmatrix} F & G^* \\ G & F^* \end{bmatrix} = \begin{bmatrix} F_R + iF_I & G^* \\ G & F_R - iF_I \end{bmatrix}, \quad (6)$$

with  $\det \mathbf{T} = 1$ . In Eq. (6),  $F^*$  and  $G^*$  denote the complex conjugates and  $F_R$  and  $F_I$  are the real and imaginary parts of  $F$ , respectively. In contrast to the characteristic matrix, the transfer matrix contains information about the refractive indices of the adjacent media.<sup>5,6</sup>

Using the parameters of coupled-mode theory, we can write the transfer matrix as<sup>15</sup>

$$\mathbf{T} = - \begin{bmatrix} \cos(\gamma) + i \frac{\delta}{\gamma} \sin(\gamma) & i \frac{\kappa}{\gamma} \sin(\gamma) \\ -i \frac{\kappa}{\gamma} \sin(\gamma) & \cos(\gamma) - i \frac{\delta}{\gamma} \sin(\gamma) \end{bmatrix}. \quad (7)$$

$\kappa$  and  $\delta$  denote the coupling and the detuning coefficients, respectively, and the effective propagation constant of the Bragg structure is equal to

$$\gamma = \sqrt{\delta^2 - \kappa^2}. \quad (8)$$

The parameters  $\kappa$ ,  $\delta$ , and  $\gamma$  are normalized to the inverse physical length of the layer combination,  $\Lambda^{-1}$ .<sup>12-14</sup> Similarly to the situation described in Subsection 2.A, passband regions are identified by real values of the propagation constant  $\gamma$ , whereas complex values indicate stop-band regions. A comparison of the transfer matrices of Eqs. (6) and (7) shows that  $F_R = -\cos(\gamma) = \cos(\gamma + \pi)$ . Thus, in the transfer-matrix formalism, the location of stop bands is completely determined by the real part of  $F$ .

As we mentioned above, the transfer matrix of Eq. (7) is exact if the coupling and detuning coefficients are properly chosen. The exact coefficients are given by<sup>12</sup>

$$\kappa = -i\alpha G, \quad (9)$$

$$\delta = -\alpha F_I, \quad (10)$$

where the factor  $\alpha$  is defined as

$$\alpha = \frac{\gamma}{\sin(\gamma)}, \quad (11)$$

with

$$\gamma = \begin{cases} -i \ln(-F_R + \sqrt{F_R^2 - 1}) & F_R < -1 \\ \arctan\left(\frac{\sqrt{1 - F_R^2}}{-F_R}\right) & -1 \leq F_R \leq 0 \\ -\arctan\left(\frac{\sqrt{1 - F_R^2}}{F_R}\right) + \pi & 0 < F_R \leq +1 \\ -i \ln(F_R - \sqrt{F_R^2 - 1}) + \pi & F_R > +1 \end{cases}. \quad (12)$$

The piecewise definition of the propagation constant  $\gamma$  allows for the distinction of different stop-band and passband regions. Complex values of  $\gamma$  (for  $|F_R| > 1$ ) define the stop bands. In the first case ( $F_R < -1$ ) the stop bands are centered at total phase shifts  $\phi$ , which are odd multiples of  $\pi$ . This includes the case of the fundamental Bragg wavelength at  $\phi = \pi$ . In the fourth case ( $F_R > 1$ ) the stop bands are centered at even multiples of  $\pi$ . It should be noted that complex values of  $\kappa$  and  $\delta$  indicate the latter case and do not identify the fundamental stop band.<sup>12</sup>

### C. Relationship between Coupled-Mode Theory and Equivalent Layers

Of the two exact descriptions of multilayer coatings introduced, one is based on the characteristic-matrix method and the other is based on the transfer-matrix method. In Eqs. (3) and (4) the equivalent-layer parameters are expressed with the elements of the characteristic matrix  $M_{ij}$ , whereas in Eqs. (9)–(12) the coupled-mode parameters are expressed with the elements of the transfer matrix of Eq. (6). We can merge the two methods by relating the elements of the characteristic matrix and the elements of the transfer matrix. If the refractive index of the adjacent media on both sides is chosen equal to the refractive index  $n_1$  of the outermost layers of the symmetrical combination of layers (see Fig. 1), the following relations are valid (see, e.g., Ref. 6):

$$F_R = M_{11}, \quad (13)$$

$$F_I = \frac{1}{2} \left( n_1 M_{12} + \frac{M_{21}}{n_1} \right) \left\{ \Leftrightarrow \begin{cases} n_1 M_{12} = F_I - iG, & (14) \\ \frac{M_{21}}{n_1} = F_I + iG. & (15) \end{cases} \right.$$

According to Eq. (13), matrix element  $M_{11}$  is now identified as the real part of transfer-matrix element  $F$ , and, in the respective formalism,  $F_R$  or  $M_{11}$  completely determines the location of stop-band and passband regions.

Using Eqs. (13)–(15), we are now able to express the equivalent-layer parameters of Eqs. (3) and (4) in terms of the transfer-matrix elements. With Eqs. (8)–(10) the equivalent-layer parameters can then be related to the coupled-mode parameters as follows:

$$N_e = n_1 \sqrt{\frac{F_I + iG}{F_I - iG}} = n_1 \sqrt{\frac{\delta + \kappa}{\delta - \kappa}}, \quad (16)$$

$$\cos(\Gamma_e) = F_R = \cos(\gamma + \pi). \quad (17)$$

When we introduce slowly varying amplitudes with respect to the total physical length,  $\Lambda$ , of the waves propagating in the right-hand direction ( $A$ ) and in the left-hand direction ( $B$ ; Fig. 1) and build the sum and the difference of these amplitudes, respectively, the coupled-mode equations are equivalent to a system of transmission-line equations.<sup>13,14</sup> For these transmission-line equations a characteristic impedance  $Z$  is defined, which is readily expressed in the parameters of the coupled-mode formalism

$$Z = \sqrt{\frac{\delta - \kappa}{\delta + \kappa}}. \quad (18)$$

This characteristic impedance is normalized to unity for the case of a vanishing coupling coefficient ( $Z = 1$  for  $\kappa = 0$ ). Substitution of Eq. (18) into Eq. (16) yields  $N_e = n_1/Z$ . Thus the equivalent index is the ratio of the refractive index of the outermost layers and the characteristic impedance.

The equivalent thickness follows from Eq. (17):

$$\Gamma_e = \pm\gamma + (2j - 1)\pi, \quad j \in \mathbb{N}. \quad (19)$$

The equivalent thickness is simply a linear function of the effective propagation constant  $\gamma$  with slope  $\pm 1$ . In Eq. (19) the plus or minus as well as  $j$  has to be chosen in accordance with the conditions stated at the end of Subsection 2.A. This yields

$$\begin{aligned} \Gamma_e &= (-1)^{\lfloor \phi/\pi \rfloor + 1} \gamma + (2j - 1)\pi, \\ \phi &\in [2\pi(j - 1), 2\pi j[. \end{aligned} \quad (20)$$

This choice is consistent with all requirements, even for complex-valued  $\Gamma_e$ .

As an example, we consider approximate coefficients from standard coupled-mode theory. In this case the detuning coefficient in the surroundings of the fundamental Bragg wavelength at  $\phi \approx \pi$  is given by  $\delta = \phi - \pi$ .<sup>14,16</sup> Moreover, in passband regions we have  $|\delta| > |\kappa|$ . Hence the effective propagation constant can be approximated by  $\gamma = |\delta|[1 + O(\kappa^2/\delta^2)] \approx |\phi - \pi|$ . With this approximation and Eq. (20), it follows that  $\Gamma_e \approx \phi$  for the passband regions at  $j = 1$ . Thus the equivalent thickness is approximately given by the total optical phase shift  $\phi$ . This result is well

known and is also valid for higher-order passbands at  $j > 1$  (see, e.g., Ref. 6). The derivation given here can easily be extended to this case.

### 3. Application to a Symmetrical Three-Layer Combination

The relations derived in Section 2 are valid for any symmetrical combination of layers. In this section we apply our results to the most important case, the symmetrical three-layer combination of Fig. 1.

According to Ref. 12, the elements of the transfer matrix are

$$F_R = \frac{1}{1 - r^2} [\cos(\phi) - r^2 \cos(\Delta\phi)], \quad (21)$$

$$F_I = \frac{1}{1 - r^2} [\sin(\phi) + r^2 \sin(\Delta\phi)], \quad (22)$$

$$G = -\frac{2ir}{1 - r^2} \sin\left[\frac{1}{2}(\phi + \Delta\phi)\right], \quad (23)$$

with

$$\phi = \phi_1 + \phi_2, \quad (24)$$

$$\Delta\phi = \phi_2 - \phi_1, \quad (25)$$

$$r = \frac{n_2 - n_1}{n_2 + n_1}. \quad (26)$$

In Eq. (26) the refractive indices of medium 1/2,  $n_{1/2}$ , define the Fresnel reflectivity  $r$ , which describes the amplitude reflectivity between the two adjacent media 1 and 2. The phase shifts  $\phi_{1/2}$  in Eqs. (24) and (25) correspond to the optical thickness of medium 1/2 expressed in phase units, as defined in Fig. 1. Thus  $\phi$  gives the total optical phase shift, whereas  $\Delta\phi$  is a measure of the duty cycle of the three-layer combination.

Substitution of Eqs. (22) and (23) into Eq. (16) and normalization of the equivalent index to the refractive index of the outermost layers leads directly to

$$\frac{N_e}{n_1} = \left\{ \frac{\sin(\phi) + r^2 \sin(\Delta\phi) + 2r \sin[(\phi + \Delta\phi)/2]}{\sin(\phi) + r^2 \sin(\Delta\phi) - 2r \sin[(\phi + \Delta\phi)/2]} \right\}^{1/2}. \quad (27)$$

From Eqs. (17) and (21) we obtain the equivalent thickness

$$\Gamma_e = \arccos\left\{ \frac{1}{1 - r^2} [\cos(\phi) - r^2 \cos(\Delta\phi)] \right\}. \quad (28)$$

The equivalent index of Eq. (27) and the equivalent thickness of Eq. (28) are identical to the results in Refs. 2–7 but are expressed in terms of Fresnel reflectivity  $r$  and phase variables  $\phi$  and  $\Delta\phi$ . These expressions are more convenient because multiple reflections can easily be classified by series expansion in  $r$ . Moreover, the mathematical structure of Eqs. (27) and (28) is simpler if these equations are ex-

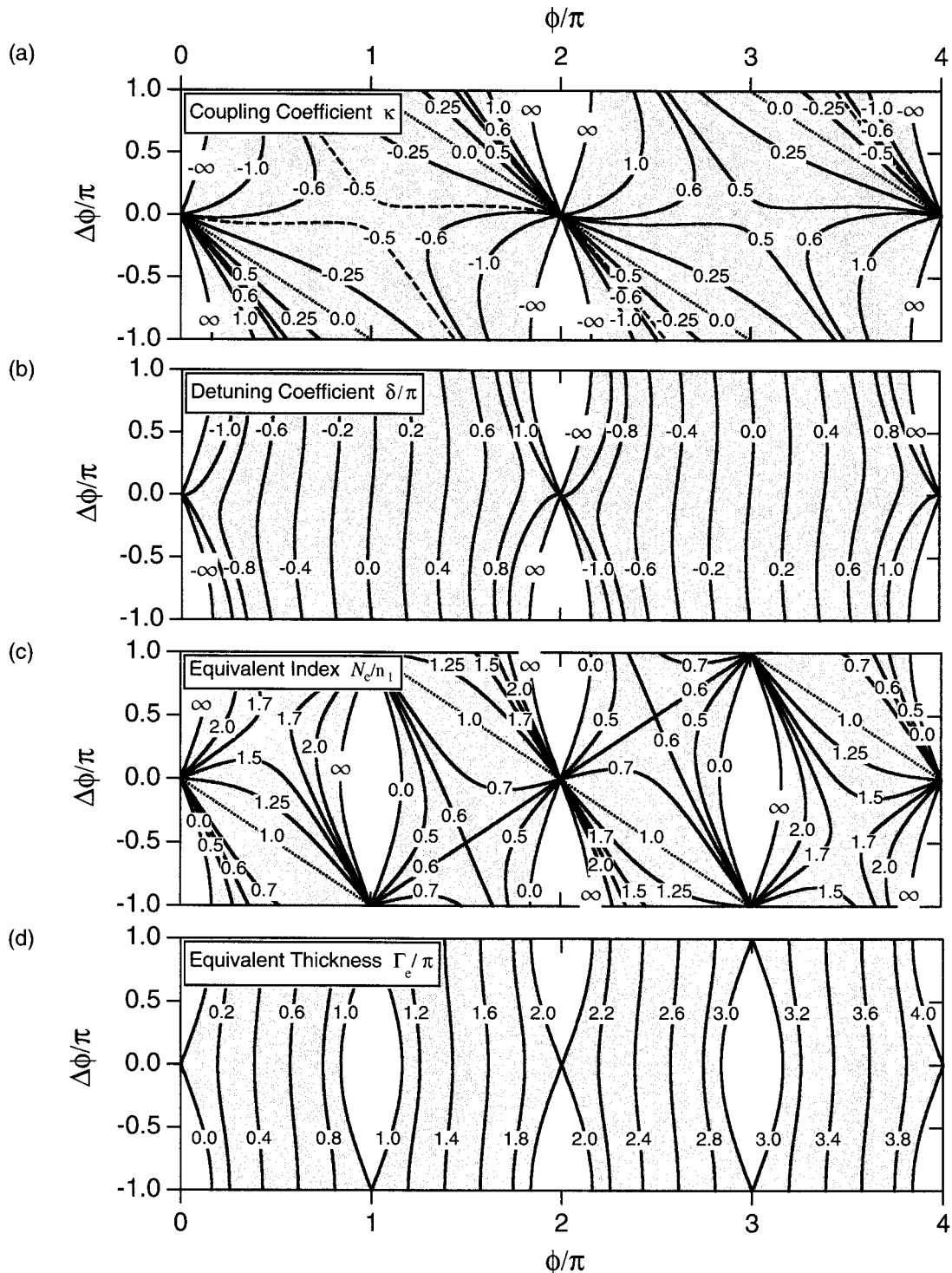


Fig. 2. Contour plots of (a) the exact coupling coefficient  $\kappa$ , (b) the exact detuning coefficient  $\delta$ , (c) the normalized equivalent index  $N_c/n_1$ , and (d) the equivalent thickness  $\Gamma_e$  as functions of the phase variables  $\phi$  and  $\Delta\phi$ . The phase variables as well as the detuning coefficient and the equivalent thickness are given in units of  $\pi$ . Shaded regions indicate real values of the parameter; white regions indicate complex parameter ranges. For the equivalent-layer parameters shown in (c) and (d), shaded and unshaded regions separate passband regions from stop-band regions. Note that only regions that fulfill the condition  $\phi \geq |\Delta\phi|$  are of physical relevance because the phase shifts,  $\phi_{1/2}$ , are positive quantities. The dashed curves in (a) are contour lines with  $\kappa = -2r = -0.5$ , the value from standard coupled-mode theory. The dotted lines in (a) and (c) are the zero contour lines of the coupling coefficient and the unity contour lines of the equivalent index, respectively. For these contour lines, medium 2 vanishes or acts as an absentee layer, as described in the text.

pressed in  $\phi$  and  $\Delta\phi$ . As an example, Eq. (28) can be approximated by  $\Gamma_e \approx \phi$  if we neglect terms of  $O(r^2)$

in the argument. This approximate result is the same as that derived above from the approximation of

the coupled-mode parameters. Physically, it is equivalent to neglecting multiple reflections within the multilayer structure. For passband regions this approximation is sufficient for many applications.

Figure 2 shows contour plots of the design parameters  $\kappa$ ,  $\delta$ ,  $N_e/n_1$ , and  $\Gamma_e$  as functions of phase variables  $\phi$  and  $\Delta\phi$ . These contour plots are similar to the plots presented by van der Laan and Frankena<sup>7</sup> for the equivalent-layer parameters as functions of  $\phi_1$  and  $\phi_2$ . The information contained in these contour plots is the same for either set of variables. The phase variables, the detuning coefficient, and the equivalent thickness are given in units of  $\pi$ . Shaded regions in the contour plots indicate real-valued parameter ranges; white regions correspond to complex parameter ranges. For the equivalent-layer parameters, shaded and unshaded regions separate passband regions from stop-band regions. In these examples we choose the refractive indices  $n_1 = 1.5$  and  $n_2 = 2.5$ , leading to  $r = 0.25$ . These values are close to the refractive indices of  $\text{SiO}_2$  and  $\text{TiO}_2$ , compounds that are used for standard laser mirrors. Note that the quantities depicted in Fig. 2 do not depend on the absolute value of refractive index  $n_1$  or  $n_2$ ; they depend only on the ratio of the indices,  $n_1/n_2$ , through Fresnel reflectivity  $r$ .

Figure 2(a) shows the exact coupling coefficient according to Eq. (9) with Eq. (23). The plot illustrates two interesting facts: First,  $\kappa \approx -2r = -0.5$  for layers with 50% duty cycle ( $\Delta\phi = 0$ ) in the vicinity of the fundamental stop band ( $\phi/\pi < 2$ ), as indicated by the dashed curves. These values compare favorably with the results from standard coupled-mode theory.<sup>16</sup> Moreover, we can see that the zero contour lines of  $\kappa$  (dotted curves) are linear functions with slope  $-1$ . According to Eq. (9), the coupling coefficient vanishes if matrix element  $G$  vanishes. This happens for  $\Delta\phi = 2\pi(j - 1) - \phi$  with  $j \in \mathbb{N}$ . Hence for  $j = 1$  the three-layer combination reduces to a single layer of material 1. For  $j > 1$  medium 2 acts as an absentee layer because its phase thickness corresponds to that of a half-wave layer or a higher-order half-wave layer.

The contour lines of the detuning coefficient, shown in Fig. 2(b), are essentially vertical lines, which illustrates the weak dependence of  $\delta$  on  $\Delta\phi$ . In the standard coupled-mode approach these lines would be exactly vertical because of their nondependence on  $\Delta\phi$ , as the approximation at the end of Section 2 shows. As discussed in Subsection 2.B, the coupled-mode parameters are complex valued only for stop-band regions near total phase shifts, which are even multiples of  $\pi$  [ $\phi = 2\pi(j - 1)$ ,  $j \in \mathbb{N}$ ].

Figure 2(c) shows the normalized equivalent index,  $N_e/n_1$ , according to Eq. (27). The zero contour lines of the coupling coefficient are transformed into unity contour lines (dotted lines) of the normalized equivalent index [cf. Figs. 2(a) and 2(c)]. Then medium 2 acts only as an absentee layer, as discussed above, and the equivalent index equals the refractive index of medium 1. According to Fig. 2(d), the equivalent thickness closely follows the value of the

abscissa, illustrating the approximation  $\Gamma_e \approx \phi$  derived above for passband regions. In the neighborhood of the stop bands, this approximation is less accurate and the deformation of the contour lines is more pronounced. Figure 2 clearly illustrates the correlation between coupling coefficient  $\kappa$  and equivalent index  $N_e$  and between detuning coefficient  $\delta$  and equivalent thickness  $\Gamma_e$ . Hence the two parameter sets are equivalent for the description of a multilayer coating.

What follows is a discussion of this equivalence in the case of a chirped mirror.<sup>17</sup> Recently we developed a theory of chirped mirrors that has resulted in the double-chirped mirror design technique.<sup>13,14,18</sup> This theory is based on the exact coupled-mode approach. As a result, it has been shown that the unwanted oscillations, which typically occur in the phase properties [group delay and group-delay dispersion (GDD)], are caused by an impedance mismatch in the front part of the mirror. We can match the impedance by properly adjusting the coupling coefficient as a function of penetration depth according to Eq. (18).<sup>13,14</sup> Furthermore, the GDD can be independently designed by proper choice of the detuning coefficient with the so-called chirp law.<sup>18</sup> In the picture of equivalent layers, the design considerations translate as follows: The oscillations in the group delay and the GDD are caused by a mismatch of the equivalent index at the mirror front. Adjusting the duty cycle of the individual three-layer combinations by means of  $\Delta\phi$  allows for broadband matching of the equivalent index within the range given by the high- and low-index materials used in the coating. Independently, the desired behavior of the GDD is achieved by proper choice of the equivalent thickness along the chirped mirror structure, which leads to a wavelength-dependent penetration depth that yields the desired dispersion.

#### 4. Conclusions

We have investigated the relationship between the method of equivalent layers and the exact coupled-mode theory. Relations between the design parameters of the equivalent layer ( $N_e$ ,  $\Gamma_e$ ) and the coupled-mode parameters ( $\kappa$ ,  $\delta$ ) have been derived. We found that the normalized equivalent index is the reciprocal characteristic impedance ( $N_e/n_1 = Z^{-1}$ ) and that the equivalent thickness is a linear function of the effective propagation constant  $\gamma$ . As a result, the coupling coefficient is strongly related to the equivalent index ( $\kappa \leftrightarrow N_e$ ); the detuning coefficient, to the equivalent thickness ( $\delta \leftrightarrow \Gamma_e$ ). These findings allow for the use of both methods (coupled-mode theory and equivalent layers) simultaneously and equivalently. This might simplify advanced analytical coating designs and provide more insight into design constraints of coatings with complex amplitude and phase properties, in particular.

This study has been supported by the Swiss National Science Foundation.

## References and Notes

1. A. Herpin, "Calcul du pouvoir réflecteur d'un système stratifié quelconque," *C. R. Acad. Sci.* **225**, 182–183 (1947).
2. L. I. Epstein, "The design of optical filters," *J. Opt. Soc. Am.* **42**, 807–810 (1952).
3. P. H. Berning, "Use of equivalent films in the design of infrared multilayer antireflection coatings," *J. Opt. Soc. Am.* **52**, 431–436 (1962).
4. A. Thelen, "Equivalent layers in multilayer filters," *J. Opt. Soc. Am.* **56**, 1533–1538 (1966).
5. H. A. Macleod, *Thin-Film Optical Filters*, 2nd ed. (Adam Hilger, Bristol, UK, 1985).
6. A. Thelen, *Design of Optical Interference Coatings* (McGraw-Hill, New York, 1989).
7. C. J. van der Laan and H. J. Frankena, "Equivalent layers: another way to look at them," *Appl. Opt.* **34**, 681–687 (1995).
8. J. R. Pierce, "Coupling of modes propagation," *J. Appl. Phys.* **25**, 179–183 (1954).
9. M. Matsuhara, K. O. Hill, and A. Watanabe, "Optical-waveguide filters: synthesis," *J. Opt. Soc. Am.* **65**, 804–809 (1975).
10. F. Ouellette, "Dispersion cancellation using linearly chirped Bragg grating filters in optical waveguides," *Opt. Lett.* **12**, 847–849 (1987).
11. H. Kogelnik and C. V. Shank, "Coupled-wave theory of distributed feedback lasers," *J. Appl. Phys.* **43**, 2327–2335 (1972).
12. N. Matuschek, F. X. Kärtner, and U. Keller, "Exact coupled-mode theories for multilayer interference coatings with arbitrary strong index modulations," *IEEE J. Quantum Electron.* **33**, 295–302 (1997).
13. F. X. Kärtner, N. Matuschek, T. Schibli, U. Keller, H. A. Haus, C. Heine, R. Morf, V. Scheuer, M. Tilsch, and T. Tschudi, "Design and fabrication of double-chirped mirrors," *Opt. Lett.* **22**, 831–833 (1997).
14. N. Matuschek, F. X. Kärtner, and U. Keller, "Theory of double-chirped mirrors," *IEEE J. Sel. Top. Quantum Electron.* **4**, 197–208 (1998).
15. In Eqs. (7)–(12) we define the elements of the transfer matrix slightly differently from the original reference (Ref. 12). In this paper we investigate the multilayer coating with respect to passband regions as the standard case. Hence the elements of the transfer matrix are expressed by trigonometric functions, unlike in Ref. 12, where the multilayer structure was investigated with respect to the fundamental stop band as the standard case. The formulas of this paper are obtained from Ref. 12 when the substitution  $\gamma \rightarrow i\gamma$  is made.
16. H. A. Haus, *Waves and Fields in Optoelectronics* (Prentice Hall, Englewood Cliffs, N.J., 1984).
17. R. Szipöcs, K. Ferencz, C. Spielmann, and F. Krausz, "Chirped multilayer coatings for broadband dispersion control in femtosecond lasers," *Opt. Lett.* **19**, 201–203 (1994).
18. N. Matuschek, F. X. Kärtner, and U. Keller, "Analytical design of double-chirped mirrors with custom-tailored dispersion characteristics," *IEEE J. Quantum Electron.* **35**, 129–137 (1999).